ACS Combinatorial Science

Technology Note

pubs.acs.org/acscombsci

Visual and Quantitative Screening of α_1-Adrenoceptor Antagonists in Living Cells Using Quantum Dots

Jing Ma,[†] Zhun Hou,[†] Yao Song,[§] Lei Wang,*[,†] and Exiang Guo*[,‡]

[†]School of Pharmacy, Shandong University, Wenhua Xilu 44, 250012 Jinan, Shandong Province, P. R. China

[‡]Qingdao Municipal Hospital, 266071 Qingdao, Shandong Province, P. R. China

[§]Institute of Vascular Medicine, Peking University Third Hospital, 49 North Garden Road, 100191 Haidian District, Beijing, P. R. China

Supporting Information

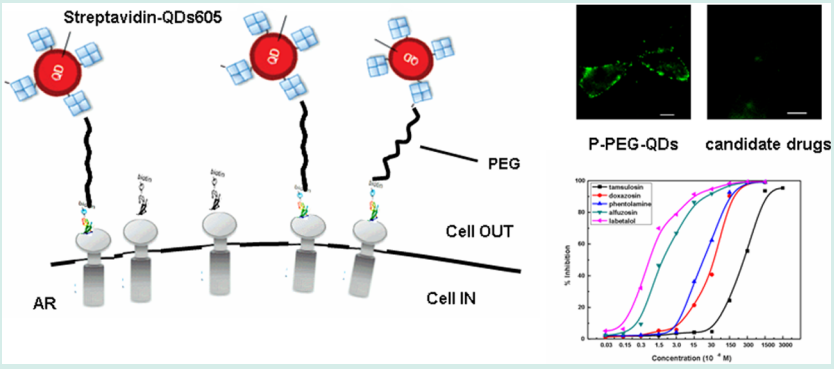

ABSTRACT: The performance of α_1-adrenoceptor antagonists in living cells was assessed using quantum dots conjugated to a derivative of the α_1-adrenoceptor antagonist prazosin. The optimum receptor binding condition and apparent K_d of prazosin-conjugated quantum dots was first determined, followed by application of these structures to drug screening. Total internal reflection fluorescence microscopy and flow cytometry were used to visually and quantitatively measure the affinity of five candidate drugs. The observed affinity order and the affinity coefficient K_i were consistent with previously reported values. These results suggest that this method is suitable for specific drug screening in living cells and is able to realize the displacement assay over the large ranges of dissociation constants.

KEYWORDS: *drug screening, quantum dots, α_1-adrenoceptor, antagonist, living cells*

G-protein-coupled receptors (GPCRs) form the largest transmembrane protein family that plays important roles in many physiological and pathological processes.[1−3] GPCRs also represent major targets of drug discovery, with over 40% of current marketed drugs acting at these cell surface receptors.[4,5] The clinical effects of most drugs are exerted by binding to receptors, and binding affinity is directly relevant to the drug activity.[6] Thus drug screening by the determination of binding with candidate compounds to the target GPCR is highly useful.

Drug screening by radioligand binding assay is efficient and accurate[7] but is inconvenient because of the use of radioactive elements under strict experimental conditions.[8] Fluorescence-based methods also have satisfactory sensitivity and resolution to monitor ligand-binding in living cells.[5] For example, Dull et al.[9] applied a green fluorescent protein tagged-glucocorticoid/estrogen receptor (GFP-GRER) chimera for live cell screening of estrogen receptor alpha (ERα) agonists and antagonists. They used an imaging system to analyze the translocation dynamics of GFP-GRER from the cytoplasm to the nucleus, which was stimulated by ERα agonists and antagonists. Stoddart et al.[5] employed a BODIPY630/650 (BY630) labeled antagonist, CA200645, to quantitatively measure the binding capacity of CA200645 to human adenosine-A1 and -A3 receptors in living cells. They further applied this probe for screening of a fragment library and identifying molecules with micromolar affinity. However, many fluorescent proteins and dyes used in these methods suffer from low photostability, and are only rarely used to provide visual and quantitative information at the same time.

Because of their unique photophysical properties, including high quantum yields, superior photostability, broad absorption spectra, narrow emission spectra, and low nonspecific adsorption, semiconductor quantum dots (QDs) have been used extensively in the study of receptor tracking,[10,11] signal transduction,[12,13] and interaction mechanisms[14] through conjugation to receptor ligands. QDs conjugated receptor ligands therefore have the potential for receptor-targeted drug screening in living cells.[15] We previously reported the synthesis of a probe in which the α_1-adrenoceptor antagonist prazosin

Received: June 12, 2013
Published: March 14, 2014

   dx.doi.org/10.1021/co5000135 | *ACS Comb. Sci.* 2014, 16, 155−159

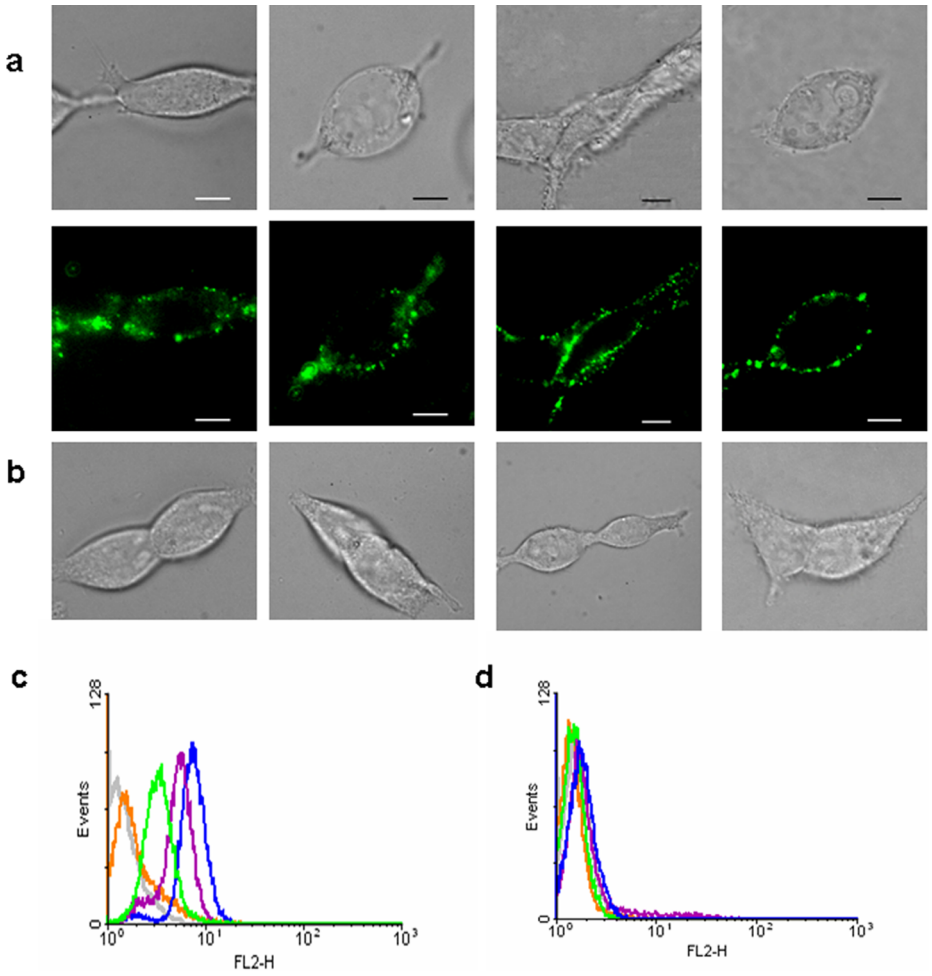

Figure 1. HEK293α_{1B} cells (a, c) and HEK293 cells (b, d) incubated with P-PEG-QDs for 15 min at 37 °C. (a, b) TIRFM images of 5, 15, 30, and 45 nM P-PEG-QDs (from left to right). Scale bar = 10 μm. (c, d) Flow cytometry measurements of 0 (gray), 5 (orange), 15 (green), 30 (purple), and 45 nM (blue) P-PEG-QDs. All events = 10 000.

was conjugated to QDs via poly(ethylene glycol) (P-PEG-QDs), and showed that the derivatized particles could specifically bind to living cells via α_1-AR in the cellular membrane.[16] Here we apply this probe for visual and quantitative screening of α_1-AR antagonists in living cells; to our knowledge, this is the first such application of QD-conjugated receptor ligands in the field of drug screening.

Human embryonic kidney 293α_{1B} cells overexpressing α_{1B}-AR (HEK293α_{1B} cells) were used as the model cell system, since the target receptor is distributed on the cell membrane surface.[17] The prazosin-derivatized P-PEG-QDs were used in live cell screening against five known antagonists of α_1-AR (labetalol, alfuzosin, phentolamine, doxazosin and tamsulosin). We employed total internal reflection fluorescence microscopy (TIRFM) and flow cytometry to visually and quantitatively study the affinity of these five candidate drugs.

The optimum binding condition of P-PEG-QDs to the receptor-bearing cells was determined by TIFRM and flow cytometry, as shown in Figure 1. Receptor occupancy increased with increasing P-PEG-QD concentration from 5 to 30 nM (Figure 1a), with no further increase at higher concentrations, suggesting that the receptor was saturated at 30 nM. HEK293 cells not displaying the characteristic of α_1-adrenoceptor displayed much reduced binding capacity to P-PEG-QDs, with no obvious fluorescence observed at 5−30 nM, and little fluorescence of P-PEG-QDs at the highest concentration. A P-PEG-QD concentration of 30 nM was therefore used in subsequent experiments.

Similar results were obtained by flow cytometry (10 000 cells, Figure 1c and d). Mean fluorescent intensity (MFI) associated with HEK293α_{1B} cells increased when the P-PEG-QD concentration was increased from 5 to 30 nM, with no further increase at 45 nM (Figure 1c). The negative control HEK293 cells showed no significant interaction with the QDs at any concentration. Three independent repetitions of this assay (Table 1) showed good consistency, and established an apparent K_d for the interaction of P-PEG-QD with the receptor-bearing cells of 1.64 ± 0.12 nM (n = 3).

Time-dependent TIRF and flow cytometry (Figure 2) measurements showed that the occupancy of the receptor was very low at the first 5 min and then increased until saturated at approximately 15 min (Figures 2a, 2c). Again, no binding was observed within 15 min between P-PEG-QDs and HEK293 cells lacking the α_{1B}-AR receptor (Figure 2b and d).

To assess the binding capacity of candidate drugs to the target receptor, HEK293α_{1B} cells were first labeled by incubation with P-PEG-QDs as above. Then the candidate drugs (labetalol, alfuzosin, phentolamine, doxazosin, and tamsulosin) were added to compete with the bound P-PEG-QDs, resulting in a loss of cellular fluorescence for ligands of

dx.doi.org/10.1021/co5000135 | ACS Comb. Sci. 2014, 16, 155−159

Table 1. Flow Cytometry Results

conditions	fluorescent intensity (mean ± SD)	
	HEK293α_{1B} cells	HEK293 cells
0 nM, 15 min	1.63 ± 0.02	1.61 ± 0.01
5 nM, 15 min	3.34 ± 0.03	1.62 ± 0.02
15 nM, 15 min	7.19 ± 0.09	1.64 ± 0.01
30 nM, 15 min	15.04 ± 0.12	1.67 ± 0.02
45 nM, 15 min	15.47 ± 0.10	2.03 ± 0.03
30 nM, 0 min	1.64 ± 0.01	1.62 ± 0.02
30 nM, 5 min	2.19 ± 0.02	1.63 ± 0.01
30 nM, 15 min	6.32 ± 0.07	1.62 ± 0.02
30 nM, 30 min	15.12 ± 0.11	1.75 ± 0.01
30 nM, 60 min	15.61 ± 0.15	2.31 ± 0.03

sufficient affinity. TIRFM images for these experiments are shown in Figure 3, in which different concentrations of candidate drugs were used after P-PEG-QDs treatment. The results show that each drug is capable of competing off the labeled quantum dots in a dose-dependent manner, and that labetalol and alfuzosin appear to be more potent than the others.

More quantitative measurements were made by flow cytometry, as shown in Figure 4. Plots of mean fluorescence intensity for each drug at a series of concentrations (0.3 nM, 1.5 nM, 3.0 nM, 15 nM, 30 nM, 0.15 μM, 0.3 μM, 1.5 μM, 3.0 μM, 15 μM, and 30 μM) gave the inhibition ratio using the formula $I = (F_p - F_d)/(F_p - F_0)$, where F_p = MFI of cells after treatment with P-PEG-QDs only, F_d = MFI after treatment with the candidate drugs following binding to P-PEG-QDs and F_0 = MFI of cells without any treatment. From these values, the

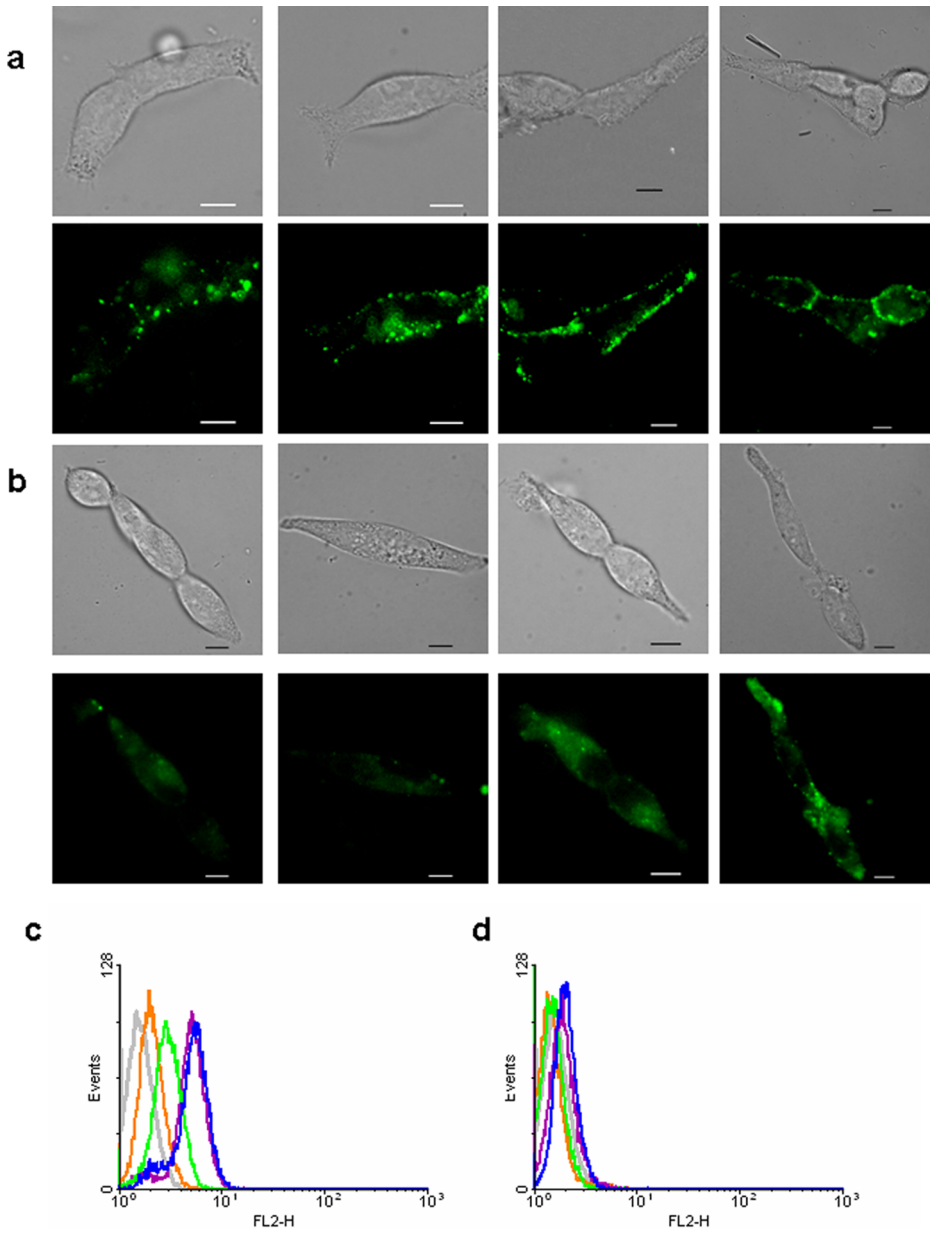

Figure 2. HEK293α_{1B} cells (a, c) and HEK293 cells (b, d) incubated with 30 nM P-PEG-QDs at 37 °C. (a, b) TIRFM images of 5, 15, 30, and 60 min (from left to right). Scale bar = 10 μm. (c, d) Flow cytometry measurements of 0 (gray), 5 (orange), 15 (green), 30 (purple), and 60 min (blue). All events = 10 000.

dx.doi.org/10.1021/co5000135 | *ACS Comb. Sci.* 2014, 16, 155−159

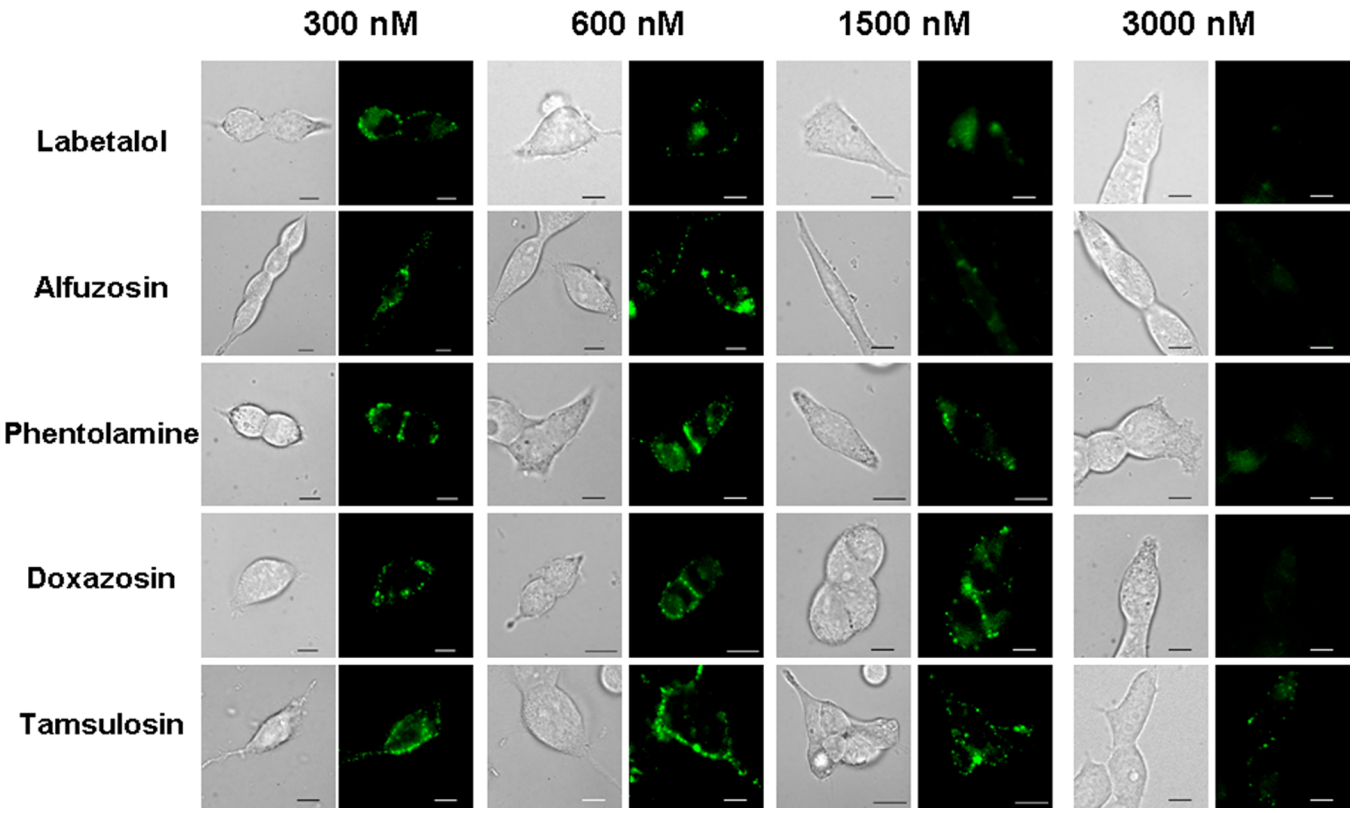

Figure 3. TIRFM images of drug competition. HEK293α_{1B} cells were treated with the indicated concentrations of candidate drugs for 15 min after treatment with 30 nM P-PEG-QDs for 15 min, all at 37 °C. Scale bar = 10 μm.

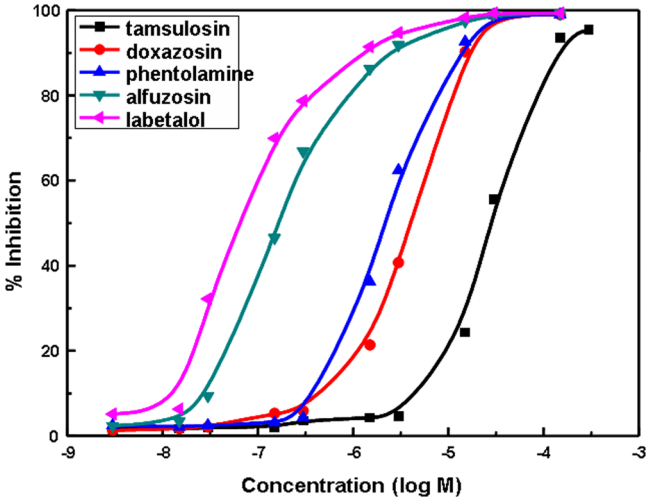

Figure 4. Inhibition ratios at cellular α_{1B}-AR for five different adrenergic antagonists.

half-maximal inhibitory concentration (IC_{50}) was calculated for each drug using SPSS software, and the binding affinity coefficient K_i determined using the formula $K_i = IC_{50}/(1 + L/K_d)$, where L = P-PEG-QD concentration (30 nM). Table 2 shows that the measured K_i values were in accordance with previously reported results using radioligand binding assays,[18−20] demonstrating the feasibility of our method.

In this assay, we successfully applied QDs conjugated to receptor ligands for visually and quantitatively measuring the binding of α_{1B}-AR antagonists to their target on living cells. The selective and ligand-dependent association of the labeled QDs with cells displaying the receptor was first established, followed by dose-dependent drug displacement monitored visually by TIRFM and quantitatively by flow cytometry. The K_i values determined in this way closely matched those in the literature, which were obtained by inconvenient radioligand displacement methods. The use of living cells ensures measurement of affinity to membrane receptors in their natural form, and the use of multivalently labeled QDs provides the fluorescence intensity and stability (both of the fluorescent signal and the cellular interaction) required for the accurate measurement of affinity constants ranging from subnanomolar to low-micromolar.

Table 2. Binding Affinities (K_i, nM) of Five Adrenergic Antagonists against α_{1B}-AR

	K_i (nM)	
drugs	measured	reference
labetalol	106 ± 6	120[20]
alfuzosin	9.4 ± 0.4	10[19]
phentolamine	7.8 ± 0.3	7.9[19]
doxazosin	1.2 ± 0.1	1.0[19]
tamsulosin	0.53 ± 0.03	0.61[18]

■ ASSOCIATED CONTENT

Ⓢ Supporting Information

Experimental procedures. This material is available free of charge via the Internet at http://pubs.acs.org.

■ AUTHOR INFORMATION

Corresponding Authors

*(L.W.) Tel: +86 531 88382330. Fax: +86 531 88565167. E-mail: wangl-sdu@sdu.edu.cn.

dx.doi.org/10.1021/co5000135 | ACS Comb. Sci. 2014, 16, 155−159

*(E.G.) Tel: +86 532 88905341. E-mail: qdgex@163.com.

Notes

The authors declare no competing financial interest.

■ ACKNOWLEDGMENTS

This project was supported by the National Natural Science Foundation of China (Grants 21175082, 21175081, 20875056).

■ REFERENCES

(1) Rosenbaum, D. M.; Rasmussen, S. G. F; Kobilka, B. K. The structure and function of G-protein-coupled receptors. *Nature* **2009**, *459*, 356−363.

(2) Hu, L. A.; Zhou, T.; Hamman, B. D.; Liu, Q. A homogeneous G protein-coupled receptor ligand binding assay based on time-resolved fluorescence resonance energy transfer. *Assay Drug Dev. Technol.* **2008**, *6*, 543−550.

(3) Liu, X.; Yue, Y.; Li, B.; Nie, Y.; Li, W.; Wu, W.; Ma, L. A G protein-coupled receptor is a plasma membrane recptor for the plant hormone abscisic acid. *Science* **2007**, *315*, 1712−1716.

(4) Lappano, R.; Maggiolini, M. G protein-coupled receptors: novel targets for drug discovery in cancer. *Nat. Rev. Drug Discov.* **2011**, *10*, 47−60.

(5) Stoddart, L. A.; Vernall, A. J.; Denman, J. L.; Briddon, S. J.; Kellam, B.; Hill, S. J. Fragment screening at adenosine-A_3 receptors in living cells using a fluorescence-based binding assay. *Chemistry & Biology* **2012**, *19*, 1105−1115.

(6) Qian, Z. M.; Li, H.; Sun, H.; Ho, K. Targeted drug delivery via the transferring receptor-mediated endocytosis pathway. *Pharmacol. Res.* **2002**, *54*, 561−587.

(7) Wang, C.; He, L.; Wang, N.; Liu, F. Screening anti-inflammatory components from Chinese traditional medicines using a peritoneal macrophage/cell membrane chromatography-offline-GC/MS method. *J. Chromatogr. B* **2009**, *877*, 3019−3024.

(8) He, L.; Yang, G.; Geng, X. Enzymatic activity and chromatographic characteristics of the cell membrane immobilized on silica surface. *Chin. Sci. Bull.* **1999**, *44*, 826−831.

(9) Dull, A.; Goncharova, E.; Hager, G.; McMahon, J. B. Development of an image analysis screen for estrogen receptor alpha (ERα) ligands through measurement of nuclear translocation dynamics. *J. Steroid Biochem. Mol. Biol.* **2010**, *122*, 341−351.

(10) Dahan, M.; Levi, S.; Luccardini, C.; Rostaing, P.; Riveau, B.; Triller, A. Diffusion dynamics of glycine receptors revealed by single quantum dot tracking. *Science* **2003**, *302*, 442−445.

(11) Wu, X.; Liu, H.; Liu, J.; Haley, K. N.; Treadway, J. A.; Larson, J. P.; Ge, N. F.; Peale, F.; Bruchez, M. P. Immunofluorescent labeling of cancer marker Her2 and other celluar targets with semiconductor quantum dots. *Nat. Biotechnol.* **2003**, *21*, 41−46.

(12) Lidke, D. S.; Nagy, P.; Heintamann, R.; Arndt-Jovin, D. J. Quantum dot ligands provide new insights into erbB/HER receptor-mediated sigal transduction. *Nat. Biotechnol.* **2004**, *22*, 198−203.

(13) Rosenthal, S. J.; Tomlinson, I.; Adlkin, E. M. Targeting cell surface receptors with ligand-conjugated nanocrystals. *J. Am. Chem. Soc.* **2002**, *124*, 4586−4594.

(14) Courty, S.; Luccardini, C.; Bellaiche, Y.; Cappello, G.; Dahan, M. Tracking individual kinesin motors in living cells using single quantum-dot imaging. *Nano Lett.* **2006**, *6*, 1491−1495.

(15) Lee, J.; Kwon, Y. J.; Choi, Y.; Kim, H. C.; Kim, K.; Kim, J.; Park, S.; Song, R. Quantum dot-based screening system for discovery of G protein-coupled receptor agonists. *ChemBioChem* **2012**, *13*, 1503−1508.

(16) Zhou, G.; Wang, L.; Ma, Y.; Wang, L.; Zhang, Y.; Jiang, W. Synthesis of a quinazoline derivative: A new α1-adrenoceptor ligand for conjugation to quantum dots to study α_1-adrenoceptors in living cells. *Bioorg. Med. Chem. Lett.* **2011**, *21*, 5905−5909.

(17) Ballou, B.; Lagerholm, B. C.; Ernst, L. A.; Bruchez, M. P.; Waggoner, A. S. Noninvasive imaging of quantum dots in mice. *Bioconjugate Chem.* **2004**, *15*, 79−86.

(18) Meyer, M. D.; Altenbach, R. J.; Basha, F. Z.; Carroll, W. A.; Drizin, I.; Elmore, S. W.; Ehrlich, P. P.; Lebold, S. A.; Tietje, K.; Sippy, K. B.; Wendt, M. D.; Plata, D. J.; Plagge, F.; Buckner, S. A.; Brune, M. E.; Hancock, A. A.; Kerwin, J. F. Synthesis and pharmacological characterization of 3-[2-((3*aR*,9*bR*)-*cis*-6-methoxy-2,3,3*a*,4,5,9*b*-hexahydro-1*H*-benz[*e*]isoindol-2-yl)ethyl]pyrido-[3′,4′:4,5]thieno[3,2-*d*]-pyrimidine-2,4(1*H*,3*H*)-dione (A-131701): A uroselective alpha 1A adrenoceptor antagonist for the symptomatic treatment of benign prostatic hyperplasia. *J. Med. Chem.* **1997**, *40*, 3141−3143.

(19) Bremner, J. B.; Coban, B.; Griffith, R.; Groenewoud, K. M.; Yates, B. F. Ligand design for α1 adrenoceptor subtype selective antagonists. *Bioorg. Med. Chem.* **2000**, *8*, 201−214.

(20) Riva, E.; Mennini, T.; Latini, R. The α- and β-adrenoceptor blocking activities of labetalol and its RR-SR (50:50) stereoisomers. *Br. J. Pharmacol.* **1991**, *104*, 823−828.